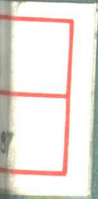


**MECHANICAL
WORKING
& STEEL
PROCESSING XXII**



MECHANICAL WORKING & STEEL PROCESSING XXII

Proceedings of the
26th Mechanical Working &
Steel Processing Conference
McCormick Center Hotel
Chicago, Illinois

Sponsored by the
Mechanical Working &
Steel Processing Division
of the
Iron and Steel Society

Lawrence G. Kuhn
Publisher

Thomas P. McAloon
Manager, Publications

Diana L. Baier
Production Manager

Melinda A. Sample
Production Assistant

698/3.1

The Iron and Steel Society, Inc.
is not responsible for statements
or opinions expressed in this
publication

Copyright ©1985
by the Iron and Steel Society, Inc.
410 Commonwealth Drive
Warrendale, PA 15086
all rights reserved

Printed in the U.S.A. by
Edward Brothers, Inc., Ann Arbor, MI 48106

ISBN No. 0-89520-166-6
Library of Congress Catalog No. 75-17963

MECHANICAL WORKING AND STEEL PROCESSING DIVISION

F.W. Irwin, *Chairman*
W.M. Wojcik, *Past Chairman*
R.B. Corbett, *Chairman-Elect*
G.S. Drigel, *Secretary*
F.C. Motts, *Treasurer*

Board Members at Large

J.M. Hambright	G.J. Roe
J.W. Young	D. Traver

Bar, Rod and Semi-Finished Products Committee

H.J. Tata and G.W. Dallin, *Co-Chairmen*

Flat Rolled Products Committee

R.M. Willison and J.K. Mahaney, Jr, *Co-Chairmen*

Roll Technology Committee

P. Horvath and W. Hogue, *Co-Chairmen*

Tubular Products Committee

T.W. Ruckman and D. Harris, *Co-Chairmen*

Process Technology Liaison Representative

J.E. Hartmann

FOREWORD

The 26th Mechanical Working and Steel Processing Conference was held in Chicago, Illinois, on the 18th and 19th of October, 1984.

This Conference is held annually in October at various locations throughout the U.S.A. and Canada.

The major objective of the Conference is to provide a forum for the presentation and dissemination of knowledge on the science and technology of the conversion processes for steel. Accordingly, the Conference provided eight technical sessions organized by its Committees on Flat Roll Products, Bars and Semi-Finished Products, Roll Technology, and Tubular Products. In addition, the Process Technology Division of ISS presented a session on the Detection of Defects at Elevated Temperatures in Metal Products. In all, a total of 32 papers were presented at the nine technical sessions. Once again, the quality of presentation and technical content was very high and provided an excellent representation of current work in both the research and operating environments in the steel industry. Our sincere thanks to all the authors for their significant contributions to the Conference.

Two plant tours were arranged for the participants of the Conference. Republic Steel Corporation provided a tour of their 32" Blooming Mill and Bar Mill Complex, and at Inland Steel the tour encompassed their 80" Tandem Mill and new Continuous Annealing Line. Our sincere thanks to both of these Corporations for providing these excellent tours.

On behalf of the Officers and Executive Committee of the Conference, I would like to thank the authors, program chairpersons, and subcommittee chairmen for the time and effort they have expended in making this Conference a success.

F.W. Irwin
Chairman - 1984
Mechanical Working and
Steel Processing Division
Iron and Steel Society

CONTENTS

原书模糊

Foreword	U
Authors' Index	297

BAR, ROD AND SEMI-FINISHED PRODUCTS I

Manganese Sulfide Inclusions in Low-Carbon Resulfurized Free-Machining Steels by <i>H. Yaguchi</i>	3
Quality Control and Development at Quanex-LaSalle by <i>D.M. Keane and P.H. Wannell</i>	13
Development of BEU Mold Design for Bottom Pouring by <i>D.C. Lamont</i>	25

BAR, ROD AND SEMI-FINISHED PRODUCTS II

Physical Modeling of Hot Deformation Processes Using Plasticine by <i>R.L. Bodnar, D.C. Ronemus, B.L. Bramfitt and D.C. Shah</i>	29
Prediction of the Structure and Mechanical Properties of Control-Cooled Eutectoid Steel Rods by <i>J. Iyer, J.K. Brimacombe and E.B. Hawbolt</i>	47

ROLL TECHNOLOGY I

Reduction of Heterogeneities in High-Carbon Cast-Steel Rolls by <i>T. Kudo</i>	61
Improving the Efficiency of Work Roll Cooling Systems by <i>R.R. Carpenter and P.J. Hannan</i>	69
Contribution of E.S.R. and Progressive Induction Hardening to the Manufacture of Deep Hardened Work Rolls by <i>C. Gaspard, P. Cosse and A. Magnee</i>	75
Mathematical Modeling System for Cold Tandem Rolling Mills: Condensed Work Roll Temperature Model by <i>J.V. Poplawski and D.A. Seccombe, Jr.</i>	89

ROLL TECHNOLOGY II

Production and Properties of HI-CR-Rolls and Their Behaviour in Cold Strip Mills by <i>W. Patt</i>	101
Use of Cast Chromium Steel Rolls in Cold-Rolling Mills by <i>U. Schmidt</i>	109
Non-Destructive Testing of Rolls for Surface Evaluation and Re-Dressing Practice by <i>R.J. Ball and D.E. Van Inwegen</i>	119

TUBULAR PRODUCTS I

Accu-Roll Mill by <i>J.A. McNally</i>	125
Centrifugally Cast Steel for Tubular Products by <i>R. L. Kumar</i>	131
Defect Avoidance in ERW Pipe Manufacture by <i>T.H. North, P.A. Koornneef and J.H. Fishburn</i>	137
On the Horizontal Continuous Casting Process for High Alloyed Stainless Tubular Goods by <i>S. Komori, E. Sunami and A. Honda</i>	153

TUBULAR PRODUCTS II

The Manufacture of Stainless Pipe of 13% and 22% Chromium Stainless Steels by the Mannesmann Rolling Processes by T. Masuda, T. Terada, T. Kawade, H. Ohtsubo, F. Togashi and T. Kurisu	163
LTV Campbell Works World Class 16" Seamless Mill by D.M. Gerstner and W. Rozmus	175

FLAT ROLLED PRODUCTS I

Design of Hot-Rolling Processes for Thick-Gauge HSLA Plate by G.E. Ruddle, D.L. Baragar and A.F. Crawley	183
Effect of Annealing Cycles on Internal Oxidation and Magnetic Properties of Electrical Steels and Their Influence on Motor Performance by G. Lyudkovsky, J.B. Barnett, P.K. Rostogi and M. Balakrishnan	197
Normalized and Tempered Bainitic Plates for API X65-X70 Pipeline Fittings by M. Pontremoli and A. Pozzi	207
Metallurgical Considerations in the Development of HSLA Steel in Automotive Wheel Steels by D.W. Dickinson, F.A. Hultgren, R.E. Mintus and J.K. Abraham	217

FLAT ROLLED PRODUCTS II

Inclusion Detection in Tin Mill Products using Magnetic Particle Method by G.R. Webster, J.M. Madritch, G.A. Perfetti and L.C. Wong	223
Effect of Hot Rolling on the Magnetic Properties of a 0.5 Si Cold-Rolled Motor-Lamination Steel by P.R. Mould and R.R. Judd	235
Tandem Mill Vibration: Its Cause and Control by D.L. Paton and S. Critchley	247
The Development and Production of an Extra Low Carbon, Aluminum Killed, Hot Dip Galvanized Steel for Improved Formability by G.S. Powley and S.L. Boston	257
Design Improvements in New Continuous Annealing Lines by M. Hoetzel	267

DETECTION OF DEFECTS AT ELEVATED TEMPERATURES IN METAL PRODUCTS - PTD SESSION I

On-Line Inspection of the Weld in Continuous Stretch Reduced Pipe by the Eddy Current Method by R.M. Harris	277
Detection of Pipe and Porosity in Hot Steel Slabs, Blooms and Billets by C.D. Rogers, B.E. Droney, J.M. Toth and H.N.G. Wadley	283
Using EMATs for High Temperature Ultrasonics by B.W. Maxfield	289

BAR, ROD AND SEMI-FINISHED PRODUCTS I

Thursday morning, October 18

Convening at 9:00 am, this session was chaired by M. Thomas, Senior Research Metallurgist, LTV Steel Company, Independence, OH, and H. Tata, Associate Research Consultant, U.S. Steel Corporation, Monroeville, PA.

MANGANESE SULFIDE INCLUSIONS IN LOW-CARBON
RESULFURIZED FREE-MACHINING STEELS

Hiroshi Yaguchi
Inland Steel Company
Research Laboratories
East Chicago, IN 46312

ABSTRACT

Manganese sulfide inclusions in continuously-cast low-carbon resulfurized free-machining steels were evaluated in terms of size, elongation and composition in order to understand the effect of steelmaking, casting and hot rolling on sulfide morphology. A comparison of the results among as-cast blooms, billets and round bars yields several observations. Their possible explanations are discussed.

INTRODUCTION

Low-carbon resulfurized free-machining steels contain a large number of manganese sulfide inclusions which gives rise to their free-machining properties. It is generally believed that a uniform distribution of large and globular sulfides is beneficial to machinability (1-4). To obtain the optimum manganese sulfide morphology in the final products, many processes such as steelmaking, casting and hot rolling should be optimized. However, the effects of these processes on manganese sulfide morphology are not fully understood. A better understanding of the factors influencing the morphology of sulfide inclusions is needed because of the recent interest in producing free-machining steels by continuous casting. This investigation was initiated to observe sulfide morphology in as-cast structure and its change during hot rolling in continuously cast free-machining steels.

MATERIALS AND EXPERIMENTAL PROCEDURES

As-continuously cast blooms of low-carbon resulfurized free-machining steels were purchased from two companies. As shown in Table I, the chemistries of Heats A and B are typical chemistries of AISI 12L14 and AISI 1215 steels, respectively. It must be noted, however, that the total oxygen content of Heat B is significantly higher than that of Heat A. The mold size of Heat B is larger than that of Heat A.

These blooms were rolled to 164 mm (6.5 inch) square billets. The finishing temperatures of Heats A and B were recorded as 930-1000°C (1700-1830°F) and 1020-1040°C (1870-1900°F), respectively. Subsequently, these billets were rolled to 71.4 mm (2.8 inch) diameter round bars. The rolling temperatures were not recorded.

Slices of as-cast blooms, 164 mm (6.5 inch) square billets and 71.4 mm (2.8 inch) round bars of both heats were secured. Microstructural observation was made on the longitudinal samples obtained from the edge, quarter and center positions. Sample size was selected so that each position from as-cast blooms, billets and round bars corresponds to one another, except for the edge position of round bars where the microstructure was measured in the plunged region for machinability test and was larger relative to the bar diameter than the same position of as-cast blooms and billets.

Using an Automatic Image Analysis System (OMNICON), sulfide inclusion size distribution and their aspect ratios (the ratio of the longest dimension to width) were measured. The number of inclusions observed in one sample was at least six hundreds. For size distribution, cross sectional areas of individual inclusions were measured, and the number of inclusions in each area category was counted. Sulfides less than 0.5 μm^2 in area were excluded from observation because of the resolution limit of the optical equipment. For aspect ratio, those of individual inclusions were measured, and then an average value was calculated. Since it has been known that the deformation of small inclusions depends on their size and that smaller inclusions are less deformed due to the inclusion matrix interfacial energy, a more strict cut-off standard was employed than the one for size measurement; namely, inclusions less than 10 μm in length were excluded (5).

An electron microprobe analyzer was used to identify inclusion chemistries. At least thirty inclusions were selected in each sample randomly, and three measurements were made in each inclusion. No measurements were made at the edge position because of the small sulfide size.

TABLE I

Chemical Analyses (w/o)

Heat	Grade	C	Mn	P	S	Si	Pb	O (ppm)
A	12L14	0.07	0.96	0.07	0.32	0.01	0.24	247
B	1215	0.06	0.83	0.07	0.34	0.011	-	407

RESULTS AND DISCUSSION

Qualitative Observation

Figure 1 shows the typical optical micrographs showing sulfide inclusions in an as-cast bloom of Heat A from each position. As expected, sulfide size at the edge position is smaller than those at other positions because of a higher cooling rate at the edge. Generally, the inclusions are more or less globular and appear along interdendritic boundaries. It appears that the inclusions in Heat A are located along interdendritic boundaries more frequently than those in Heat B. This behavior is probably due to the higher oxygen content in Heat B, since it has been known that oxygen increases the tendency of sulfides to nucleate in liquid form (6). This probably results in earlier sulfide nucleation during solidification and thus more random distribution. In addition, a fine network of sulfide inclusions was occasionally observed mainly at the center position as shown in Fig. 1(c). This network has been observed previously and suggested that it is outlining prior austenite as a result of precipitation during cooling (7-9).

Iron sulfide phase was found mainly at the center position especially at the location where sulfide inclusions were concentrated. This observation indicates that at the final stage of solidification, the manganese to sulfur ratio is reduced due to the accumulating concentration of sulfur in the liquid and the slow diffusion rate of manganese in solid phase. The volume fraction of iron sulfide phase was higher in Heat B than Heat A because of the smaller manganese to sulfur ratio.

Three dimensional inclusion morphology was observed in the SEM after heavily etching in 50% nitric acid - 50% methyl alcohol solution. Typical examples are shown in Figure 2. This

observation and optical microscopy indicate that most of the sulfide inclusions were classified as of Type I according to the Sims' classification, although a significant number of elongated and segmented inclusions were detected (10). These qualitative observations in as-cast blooms reveal that sulfide inclusion morphology in continuously cast steels is similar to that in ingot cast steels (6,10,11).

Figures 3 and 4 show the typical sulfide inclusions in billets and round bars of Heat A, respectively. As expected, inclusions were elongated along the rolling direction with elongation of inclusions in round bars being larger. Iron sulfide phase, on the contrary to as-cast blooms, was rarely observed in billets and never in round bars.

Microprobe Observation

Microprobe analyses of sulfide inclusions were carried out. Since no significant difference was found between the quarter and center positions, the average values were obtained and are listed in Table II. As mentioned before, no measurements were made at the edge position because inclusions were too small to measure accurately. The results show that, as is well known, manganese sulfide inclusions are not stoichiometric but contain a significant amount of iron. It has been pointed out that the iron content of sulfide inclusions in as-cast samples depends on cooling rate, and that a higher iron content is associated with a more rapid cooling rate (12,13). The iron content of sulfides in as-cast samples made in ingots has been reported to be between three and seven percent (13,14). The iron content was higher in Heat B, and it is probably due to the lower manganese to sulfur ratio in Heat B in spite of the larger mold size and somewhat slower solidification rate. Oxygen was not detected in

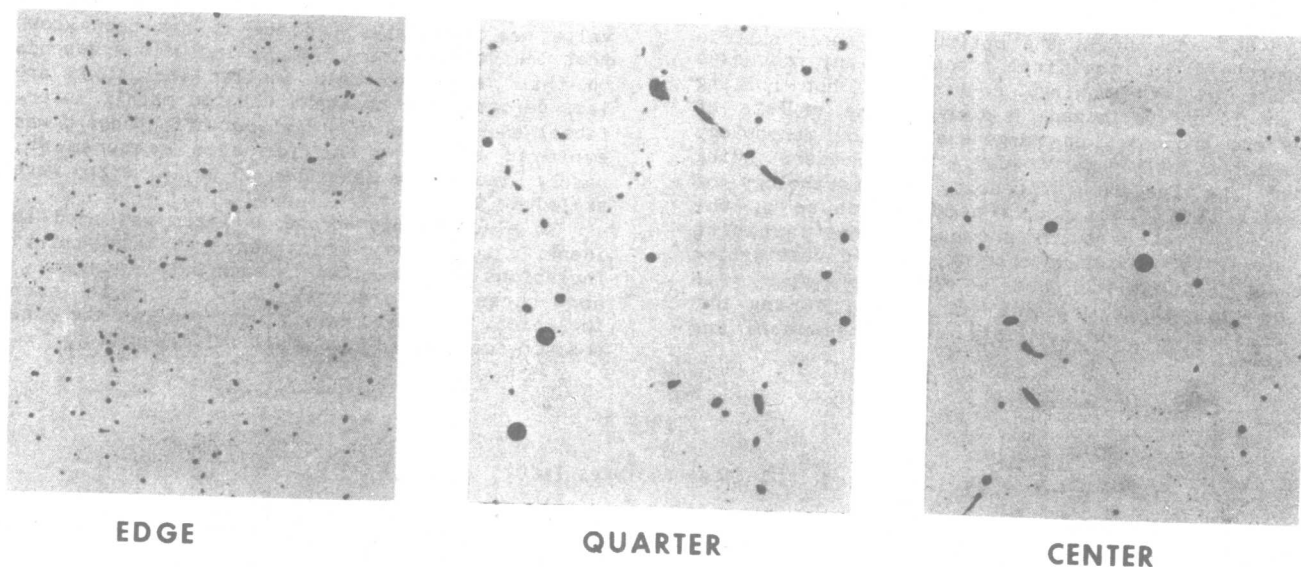
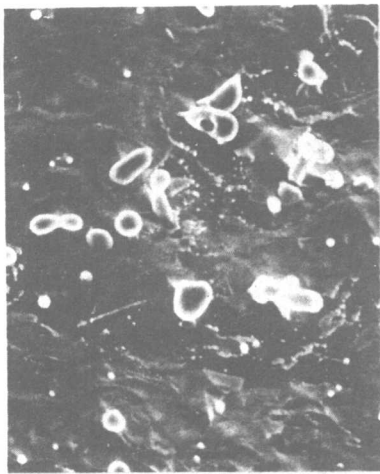
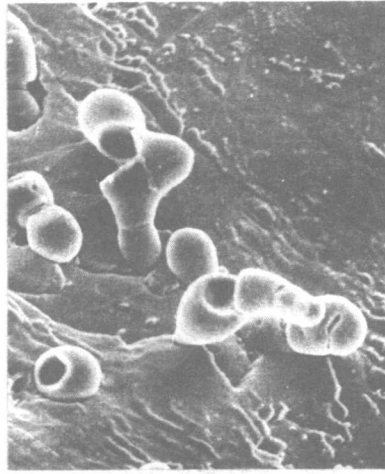


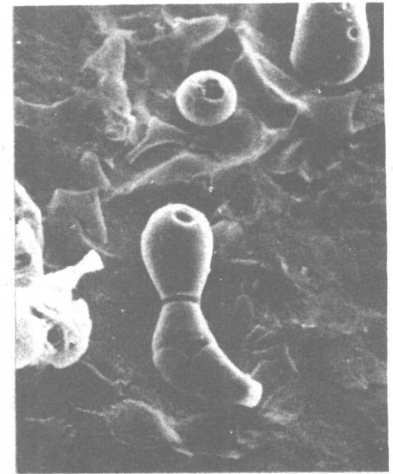
Figure 1 As-Cast Microstructures of Heat A, 260 X.



(a)
EDGE
920X

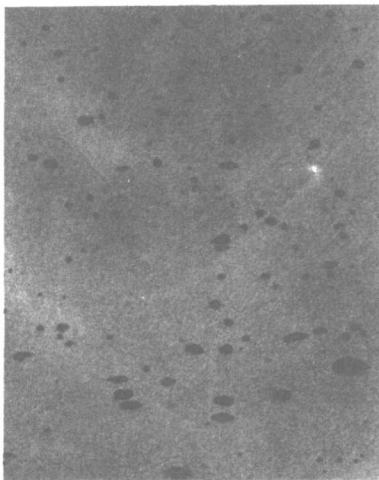


(b)
QUARTER
880X

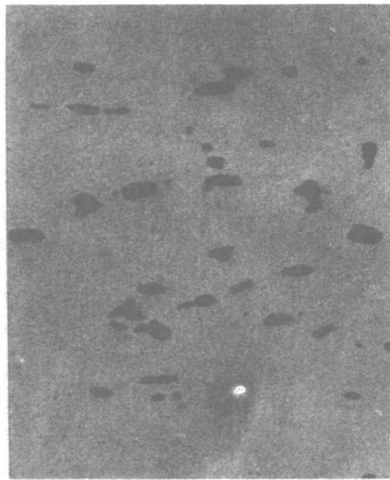


(c)
CENTER
880X

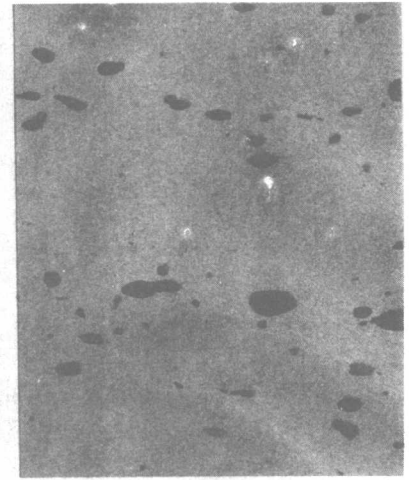
Figure 2 SEM Micrographs of As-Cast Inclusions in Heat B.



EDGE



QUARTER



CENTER

Figure 3 Microstructures of Heat A in Billet, 260 X.

amounts greater than the detectability limit in any sulfides. However, it must be noted that the detectability limit could be as high as a few weight percent.

Sulfide inclusion composition changed during rolling as predicted thermodynamically (15). As shown in Table II, the sulfur content is constant, while the manganese content increases, and the iron content decreases as the rolling process proceeds. Diffusion of iron and manganese takes place mainly during the initial stage of rolling, from bloom to billet.

Occurrence of diffusion can also be recognized from the observation mentioned above that iron sulfide phase found in as-cast structure was not detected in rolled products as was reported previously (7,11).

Inclusion Size Measurement

Figures 5, 6 and 7 show the inclusion size distribution curves of Heat A in as-cast blooms, billets and 71.4 mm (2.8 inch) round bars, respectively. The number of inclusions in each

TABLE II
Summary of Microprobe Analyses (w/o)

Heat		Si	S	Mn	Fe	Cr	Percentage Reduction of Fe
A	As-Cast Bloom	0.2 +0.1	34.7 +0.1	50.8 +1.3	14.2 +1.4	-	-
	Billet	<0.1	34.2 +0.1	60.9 +0.3	4.7 +0.2	-	67%
	71.4 mm Round Bar	0.3 +0.1	34.5 +0.1	59.8 +0.2	4.1 +0.2	-	71%
B	As-Cast Bloom	<0.1	34.9 +0.1	49.1 +0.8	16.0 +0.9	<0.1	-
	Billet	<0.1	34.7 +0.1	59.4 +1.0	6.9 +1.0	-	57%
	71.4 mm Round Bar	<0.1	34.8 +0.1	60.3 +0.3	4.6 +0.3	-	71%

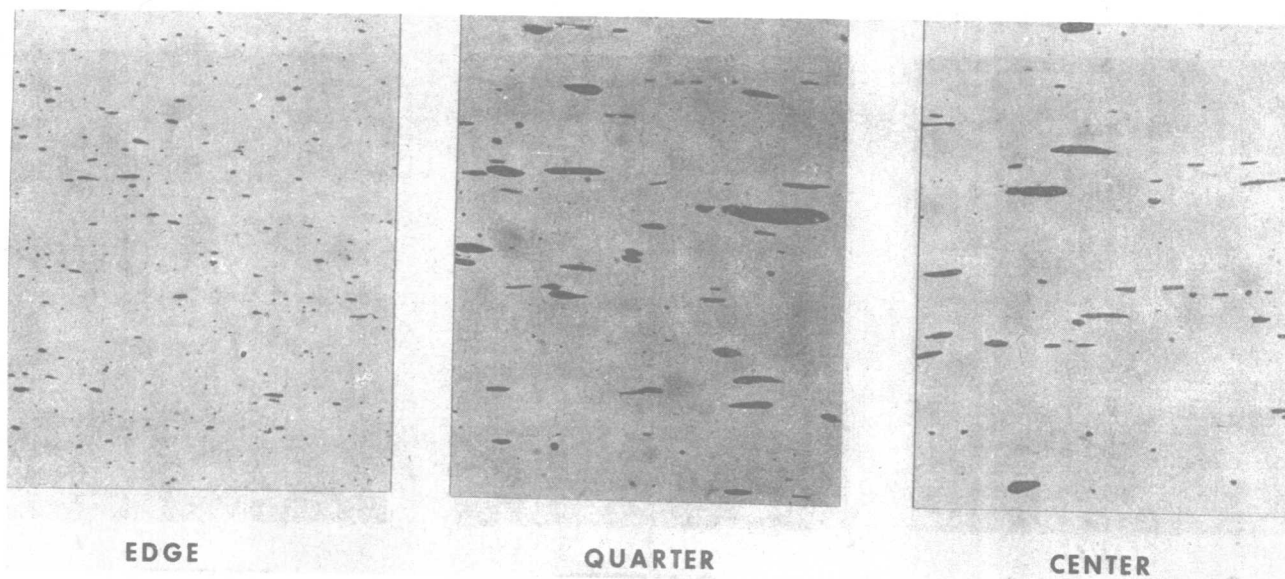


Figure 4 Microstructures of Heat A in 71.4 mm Round Hot Rolled Bar at 260 X.

area category per unit area is plotted as the ordinate, and area per inclusion as the abscissa. The results of Heat B are similar to Figs. 5, 6 and 7, and thus are not shown here. It must be noted that although oxide inclusions and lead particles were occasionally included in measurement, they are considered to be insignificant. Thus, these data can be regarded as the sulfide inclusion size distribution.

Several observations can be made from these curves. Firstly, the number of inclusions generally decreases with inclusion size. However, a peak at small inclusion size, around $2 \mu\text{m}^2$, is observed at all the positions of as-cast

blooms, Fig. 5. In addition, another peak or shallow slope region is observed at the medium inclusion size at the quarter and center positions. The presence of the secondary peak could indicate that a large number of sulfide inclusions were nucleated under the same condition. Since it is well known that Type I sulfides are nucleated as liquids in the liquid metal between the dendrite arms, the inclusion size of the secondary peak could suggest the dendrite arm spacing and thus the solidification rate when the steel chemistries are equivalent (6,10). A comparison between two heats reveals, as shown in Fig. 8, that the inclusion size of

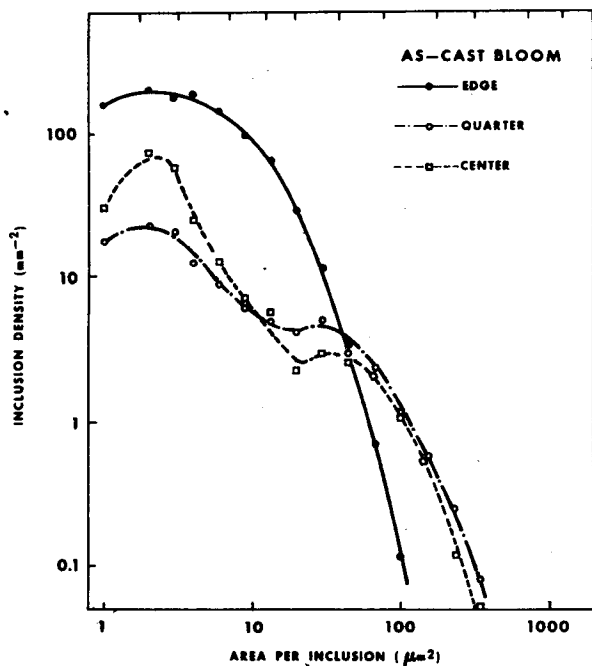


Figure 5 Inclusion Size Distribution Curves in As-Cast Bloom of Heat A.

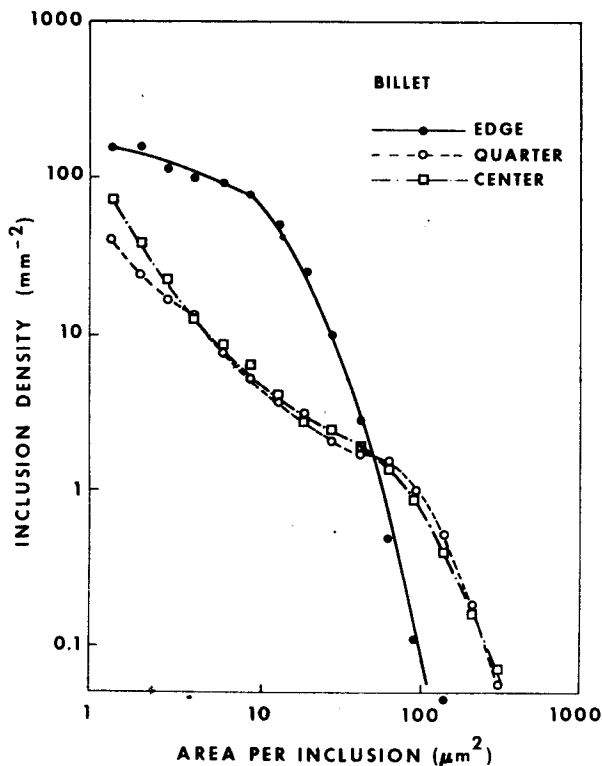


Figure 6 Inclusion Size Distribution Curves in Billet of Heat A.

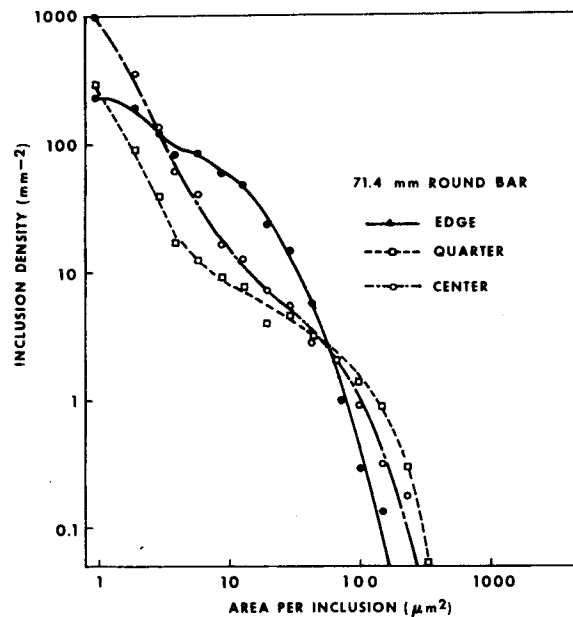


Figure 7 Inclusion Size Distribution Curves in 71.4 mm Round Hot Rolled Bar of Heat A.

the secondary peak is larger for Heat B than for Heat A. This observation is in accordance with the expected slower solidification rate in Heat B due to the larger mold size.

Secondly, as observed microscopically, the inclusion size at the edge position is significantly smaller than those at other positions because the number of large inclusions at the edge is substantially small. A comparison between the quarter and center positions reveals that the number of large inclusions is generally larger at the quarter than at the center, and that the number of small inclusions is, on the contrary, less at the quarter. In other words, the inclusion size at the quarter position is maximum of three positions. This statement is further supported by the comparison of average inclusion size shown in Table III. Two kinds of average values were calculated. One includes all the measured inclusions, and the other, shown inside of parentheses, is recalculation with inclusions less than $10 \mu\text{m}^2$ in area excluded. The purpose of obtaining two average values is to evaluate the effect of small inclusions on the average values.

Two more observations can be made from Table III. Firstly, inclusion size of Heat A is smaller than that in Heat B at the quarter and center positions. This phenomenon is in accordance with the inclusion size comparison at the secondary peak in sulfide size distribution curves. Thus, it can be stated that the secondary peak is a useful method to compare the inclusion size. On the contrary to these two positions, the sulfide size at the edge is almost equivalent.

Next, it must be noted that the average sulfide inclusion size including all the inclusions decreases as rolling proceeds at the quarter and center positions. The increase of

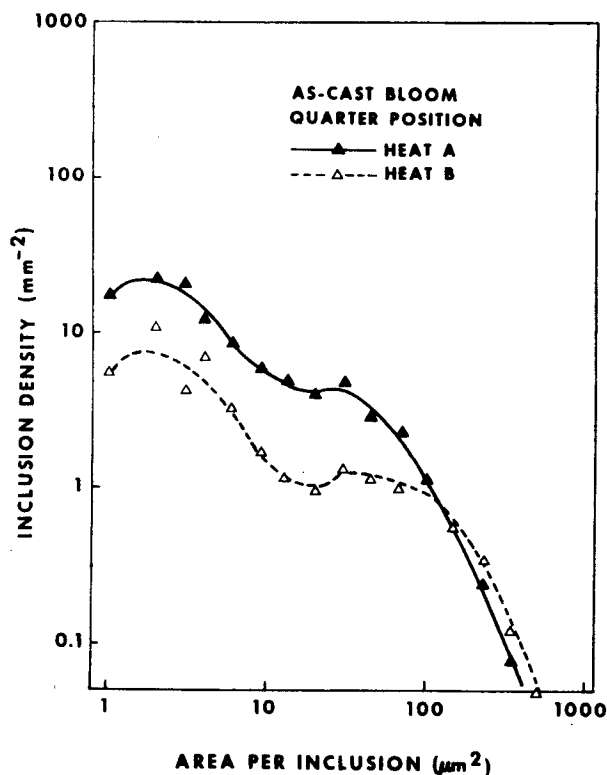


Figure 8 Inclusion Size Distribution Curves in the Quarter Position of As-Cast Blooms - Comparison Between Heat A and Heat B.

sulfide size at the edge is not considered to be a real phenomenon, because the relative sample size of round bars compared with the bar diameter is much larger than those of as-cast blooms and billets. In other words, the edge position of round bars includes not only the real edge position but also somewhat deeper positions.

Initially, this phenomenon was considered to be due to the breaking-up of large inclusions during rolling. However, when small inclusions are excluded from average size of the quarter and center positions, they do not differ significantly among as-cast blooms, billets and round bars as shown in Table III. Moreover, a comparison of sulfide size distribution curves reveals that the number of large inclusions did not decrease. On the contrary, the number of small inclusions increased significantly. Typical inclusion size distribution curves of as-cast blooms and round bars of Heat A at the quarter position are shown in Fig. 9. In order to identify the origin of these small inclusions, two pieces were cut from the quarter and center positions of an as-cast bloom of Heat A and heat treated at 1205°C (2200°F) for 2.5 hours in argon atmosphere. The inclusion size distribution curve after heat treatment at the quarter position is superimposed on those of the as-cast bloom and round bar in Fig. 9. It can be seen that the number of small inclusions increased significantly during heat treatment as well as during hot rolling. Since measurements at the center position yielded the same results, it can be concluded that breaking-up of large inclusions is not the main cause of the reduction in average inclusion size but small inclusions literally appeared during

TABLE III

Manganese Sulfide Inclusion Size (μm^2) Inside of Parentheses are Recalculated Average Value with Excluding Inclusions Less than $10 \mu m^2$ in Area

	Heat A		
	As-Cast Bloom	Billet	71.4 mm Round Bar
Edge	8.7 (19.1)	9.8 (18.7)	10.8 (23.9)
Quarter	50.6 (67.8)	53.3 (76.5)	28.0 (68.6)
Center	36.3 (69.7)	47.4 (75.4)	9.6 (53.7)

	Heat B		
	As-Cast Bloom	Billet	71.4 mm Round Bar
Edge	7.2 (19.3)	9.9 (20.3)	15.2 (38.5)
Quarter	88.1 (112.2)	49.2 (102.7)	30.7 (126.6)
Center	62.6 (110.9)	39.3 (88.1)	28.7 (118.1)

hot rolling. This observation also excluded the possibility that the increase of the number of small inclusions is an artifact due to the fact that the observed inclusion distribution curve is a function of inclusion elongation.

Optical metallography suggests from their colors, that most of the small inclusions which appeared during heat treatment are manganese sulfide inclusions. Limited number of SEM and STEM observations also support this. It has been known that sulfide inclusions precipitate in various kinds of steels after heating them above a certain temperature (17,18). This investigation confirms that sulfide precipitation and coarsening also take place in low carbon resulfurized free-machining steels. It has been observed that a small number of sulfide inclusions precipitates during cooling after casting especially at prior austenite grain boundaries as shown in Fig. 1(c). However, majority of precipitation took place during reheating.

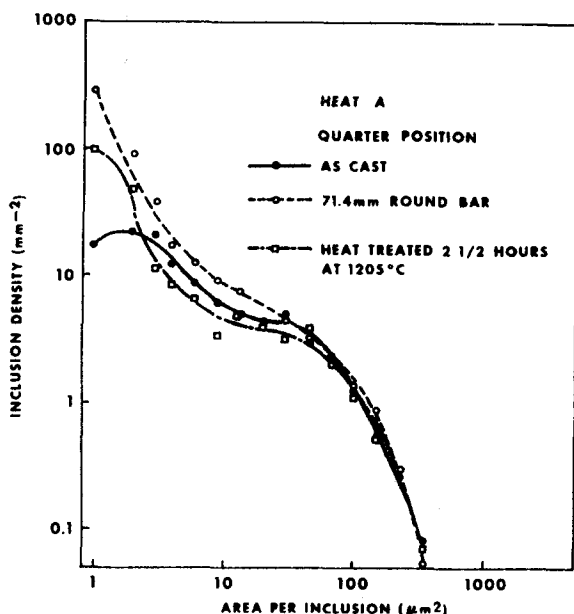


Figure 9 Inclusion Size Distribution Curves in the Quarter Position of Heat A Showing the Effect of Heat Treatment.

Sulfide Deformation Behavior

The aspect ratio of inclusions, the ratio of the longest dimension to the width, was employed as a parameter to evaluate sulfide deformation behavior. The results are listed in Table IV. As expected, the aspect ratio in round bars is greater than that in billets. It can also be observed that inclusions in Heat A were more elongated than those in Heat B.

Since the rolling reduction ratios from bloom to billet and from billet to round bar are different, this difference must be taken into account in comparing sulfide deformability. According to Malkiewicz and Rudnik, the index of deformability (v) for inclusions is given by

$$v = \frac{2}{3} \frac{\ln \lambda_2 - \ln \lambda_1}{\ln h}$$

where λ_1 and λ_2 are aspect ratios of the inclusions before and after reduction, respectively, and h is the steel reduction ratio in area (19). The aspect ratio in as-cast blooms is assumed to be one, although elongated inclusions were observed as shown in Figs. 1 and 2, because the directions of elongation are random. The results from bloom to billet, and from billet to round bar are tabulated in Table V.

Three interesting results can be observed: 1) the deformability indices from bloom to billet are higher than those from billet to round bar, 2) the deformability indices for Heat A are always higher than those for Heat B, and 3) the deformability indices of the edge position are larger than those of the quarter and center positions during rolling from bloom to billet; whereas, they become smaller than those of other two positions during rolling from billet to round bar.

Before discussing the possible mechanism for these three phenomena, it seems beneficial to summarize the four theories in the literature on sulfide inclusion deformation during hot rolling:

- 1) The ratio of the hardness of sulfide inclusions to that of the matrix influences sulfide deformability. The fact that sulfide deformation decreases with increasing rolling temperature can be interpreted by the increase of the ratio of hardness, despite the fact that the hardness of sulfides themselves decreases with temperature (20).

TABLE IV

Aspect Ratio

	Heat A		Heat B	
	Billet	71.4 mm Round Bar	Billet	71.4 mm Round Bar
Edge	4.35	6.00	3.90	4.41
Quarter	3.11	6.48	2.86	4.73
Center	3.07	6.85	3.03	4.68

TABLE V
Deformability Index

	Heat A		Heat B	
	Bloom ↓ Billet	Billet ↓ 71.4 mm Round Bar	Bloom ↓ Billet	Billet ↓ 71.4 mm Round Bar
Edge	0.895	0.113	0.604	0.043
Quarter	0.690	0.258	0.467	0.176
Center	0.682	0.282	0.492	0.153
Average	0.764	0.213	0.525	0.121

- 2) The interaction between the inclusion and the matrix influences inclusion deformability (20). The non-uniform deformation of the matrix around the inclusion, resulting from the previous deformation, restricts further deformation when the inclusions have low plasticity. In addition, the increase of the interfacial area due to deformation also restricts further deformation when the inclusions are initially highly deformable.
- 3) High levels of oxygen content promote the formation of globular sulfides. The presence of dissolved oxygen and/or manganese oxide in the manganese sulfides probably restrict the amount of their deformation (21,22).
- 4) High levels of iron content of sulfide inclusions increase their elongation (4,12).

The deformability difference between Heats A and B cannot be interpreted by the iron content of sulfides, because the results of microprobe analyses show that sulfide inclusion chemistries are almost the same. As mentioned before, the finishing temperature of Heat A blooms were low, and this may be the reason for the large deformability index for Heat A. However, it is unlikely that the rolling temperature from billet to final product for Heat A was also significantly low. It must be noted that the total oxygen content for Heat B is significantly higher than that for Heat A. This is shown in Table I. Thus, it seems reasonable to conclude that the larger deformability index of Heat A than for Heat B is most likely due to the lower oxygen content.

The rolling temperature from billet to final product is equal to or lower than that from bloom to billet. If lower, this difference could influence sulfide deformability. However, according to Baker and Charles, sulfide deformability decreases with temperature in the range 900-1200°C (1650-2190°F), which is

contrary to the results of this investigation, see Table V (20). A reduction of inclusion deformability with increasing degree of deformation has been reported by many investigators (16,19,20). This has been attributed to the interaction effect between inclusion and matrix. The results of this investigation can also be interpreted by this mechanism. However, the iron content of sulfides may also be important because the iron content of sulfides decreases as rolling proceeds.

Somewhat different sulfide deformation behavior at the edge position from other positions has also been reported previously by Clayton and Brown (23). However, in contrast to this investigation, sulfides at the edge position were found to be elongated mainly during rolling from billet to round bar rather than from bloom to billet. The results of Clayton and Brown are rather surprising because it was also observed that sulfides at the edge position appeared green or yellow under transmitted polarized light. Generally, stringer type sulfides appeared green and globular sulfides red in other positions. The reason for discrepancy between the results of Clayton and Brown and those of this investigation is not known at this time. However, it seems that the inclusion cut-off size for the aspect ratio measurement in an Automatic Image Analysis System is important because, as it has been mentioned, smaller inclusions are less deformed due to the interfacial energy. Since a large number of sulfide inclusions at the edge position is smaller than the cut-off size employed in this investigation, a significant difference is expected in the average aspect ratio between the measurements with and without employing cut-off.

CONCLUSIONS

Manganese sulfide inclusions in continuously-cast free machining steels were evaluated in as-cast blooms, billets and round bars. The following conclusions can be made:

- 1) Sulfide inclusions observed in as-cast blooms are basically of Type I with a significant